Electronic Supplementary Information (ESI)

Guest Effect on Crystal Structure and Phosphorescence of a Cu_6L_3 Prismatic Cage

Zhi-Chun Shi,[a,b,†] Wei Chen,[b] Shun-Ze Zhan,[b] Mian Li,[b] Mo Xie,[a] Yan Yan Li,[a] Seik Weng Ng,[c] Yong-Liang Huang,[a] Zhiyin Zhang,[a] Guo-Hong Ning,*[a] Dan Li*[a]

[a] College of Chemistry and Materials Science, Jinan University, Guangzhou 510632, P. R. China

[b] Department of Chemistry, Shantou University, Guangdong 515063, P. R. China

[c] Department of Chemistry University of Malaya, Kuala Lumpur, Malaysia.

[†]Present address: Department of Chemistry and Biochemistry and Biomolecular Sciences Institute, Florida International University, Miami, Florida 33199, United States.

Table of Contents

1. Experimental information

All reagents and solvents were purchased and used without further purification. Thermogravimetric analysis (TGA) was carried out in a nitrogen stream using Q50 TGA (TA) thermal analysis equipment with a heating rate of 10 °C min^{-1}. ^1H NMR spectra were recorded on Bruker Biospin Avance (400 MHz) equipment. Powder X-ray diffraction (PXRD) patterns of bulk samples were measured on a Bruker D8 Advance diffractometer (Cu Kα) under room temperature. The solid-state UV-vis spectra were measured as KCl disks with a Bio-Logic MOS-450/AF-CD Spectrometer. Infrared spectra were obtained as KBr disks on a Nicolet Avatar 360 FT-IR spectrometer in the range of 4000−400 cm^{-1} (abbreviations for the IR bands: w = weak, m = medium, b = broad, and vs = very strong). Elemental analyses were carried out with an Elementar vario EL Cube equipment. The steady-state photoluminescence spectra (PL) and the lifetime (Decay) measurements for all samples were recorded on a PTI QM/TM spectrofluorometer (Birmingham, NJ, USA). Corrections of excitation and emission for the detector response were performed ranging from 200−900 nm. Absolute quantum yield was recorded by Hamamatsu C11347-01 absolute PL quantum yield spectrometer under room temperature.

1.1. Synthesis of ligand

H_2L (4,4'- thiophene-bisethylene)-bis-diethylpyrazole)

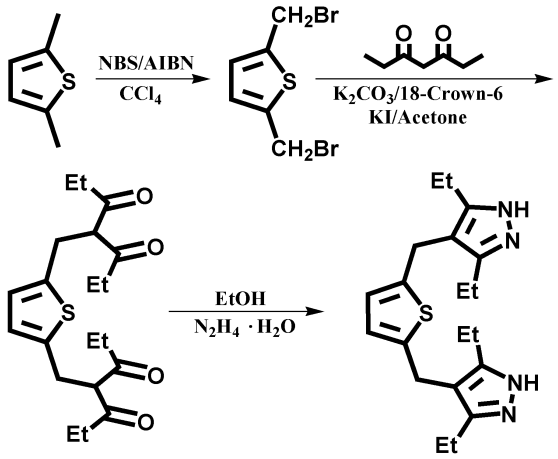

Figure S1. Synthesis of the ligand **H_2L**.

2,5-Bis(bromomethyl)thiophene was prepared according to the reported method[1] with slight modification. A mixture of 2,5-dimethylthiophene (52.2 mmol, 6.0 mL) and N-Bromosuccinimide（NBS, 113 mmol, 20.0 g) in CCl_4 (170 mL) was induced with recrystallized azobisisobutyronitrile（AIBN, 500 mg) and refluxed under N_2 atmosphere for 17 hours. The resulting mixture was filtered and the solution evaporated to dryness by rotary evaporators. The solid residue was recrystallized from hexane. The recrystallized 2,5-Bis(bromomethyl)thiophene was separated by vacuum filter, yield 60%. ^1H NMR (400 MHz, $CDCl_3$, 298 K), δ (ppm) 4.66 (s, 4H, CH_2), 6.93 (s, 2H, CH_{thio}).

Potassium carbonate (11.4 g, 80 mmol), 18-cromw-6 (1.3 g, 5 mmol) were added into a

flask with acetone (100 mL), then stirred for 15 minutes at room temperature under the protection of N_2 atmosphere, and then 3,5-heptanedione (8.15 mL,60 mmol) was added and continuously stirred. After 30 minutes, the 2,5-bis-(bromomethyl)-thiophene (5.0 g, 18.29 mmol) was added in 15 minutes after it was filtered. The reaction mixture was stirred and heated at 85 °C for 20 h. The oil residue was obtained when the organic solvent was removed under reduced pressure, washed with water, then extracted with CH_2Cl_2, dried with Na_2SO_4. The reddish-brown oil was collected, and purified by column chromatography (eluent: petroleum ether/ether acetate = 8/1, v/v), and light-yellow oil was obtained.

Then hydrazine hydrate (10 ml, 98 %) was added to the ethanol solution (100 ml) of the light-yellow oil, the solution was stirred and refluxed at 80 °C for 12 h. 4,4'- thiophene-bisethylene)-bis-diethylpyrazole (**H_2L**) was obtained as precipitate in 1.8 g after removal of all solvent. (yield 27%, based on 2,5-bis(bromomethyl)thiophene). ^{1}H-NMR (400 MHz, $CDCl_3$, 298 K): δ (ppm) 6.47 (s, 2H, CH_{thio}), 3.81 (s, 4H, CH_2), 2.56 (q, 8H, J = 8 Hz, CH_2), 1.17 (t, 12H, J = 8 Hz, CH_3). IR spectrum (KBr pellets, cm^{-1}): 3517.56 (w), 3414.78 (w), 3328.56 (w), 3197.13 (w), 3129.38 (w), 3074.86 (w), 2920.63 (b), 1721.42 (w), 1633.37 (m), 1580.38 (m), 1458.12 (s), 1375.10 (m), 1289.39 (b), 1235.09 (w), 1123.94 (w), 1071.99 (w), 1041.70 (s), 959.49 (m), 906.28 (w), 798.50 (s), 488.82 (w). Elemental analysis (CHN), $C_{20}H_{28}N_4S_3$, calculated (%): C 57.11, H 6.71, N 13.32; found (%): C 57.19, H 6.58, N 13.50.

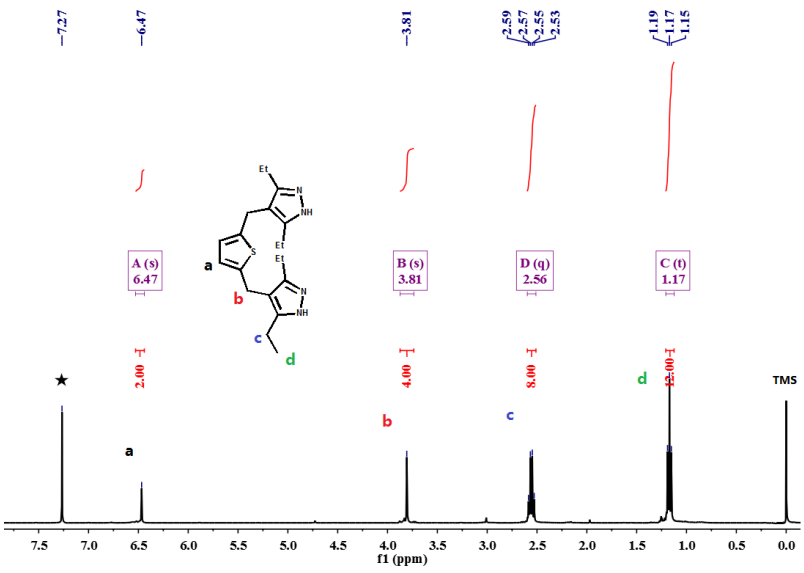

Figure S2. ^{1}H NMR (400 MHz, CDCl3, 298 K) spectra of **H_2L**

1.2 Synthesis of inclusion complexes

Caution! The volume of solution should not exceed half of the volume of Pyrex tube to avoid overloading in solvothermal synthesis.

The single crystals of inclusion complexes were obtained in a straightforward way by reacting stoichiometric amounts of Cu(I), H_2L and the corresponding aromatics *via* solvent thermal reaction, which similar to the methods reported by us before.

General method: A mixture of Cu_2O (10 mg, 0.07 mmol), **H_2L** (25.0 mg, 0.073 mmol), and mixed solvent benzene (Ph)/acetonitrile (2 mL, 1:1, v/v) was sealed in a Pyrex glass tube and heated in an oven at 140 °C for 72 hours and was cooled to room temperature with a cooling rate of 5 °C per hour. Colorless block crystals of inclusion complexes **1⊃Ph** were filtered off and dried in a vacuum oven at 80 °C for 12 hours. (6.2 mg, yield 15.9 %, based on Cu). IR spectrum (KBr pellets, cm^{-1}): 3435.65 (m), 3052.01 (w), 2963.88 (vs), 2923.99 (m), 2868.23 (m), 1637.16 (w), 1537.95 (s), 1505.25 (s), 1436.30 (s), 1368.23 (s), 1303.19 (m), 1246.58 (w), 1206.11 (s), 1151.79 (w), 1055.31 (vs), 1028.03 (m), 974.73 (w), 918.80 (w), 792.17 (s), 670.98 (vs), 513.86 (w). ^{1}H NMR (400 MHz, CD_2Cl_2, 298 K): δ (ppm) 7.28 (s, 6H, Ph-H), 6.64 (s, 6H, CH_{thio}), 3.79 (s, 12H, CH_2), 2.57 (q, 24H, CH_2), 1.11 (t, 36H, CH_3). Elemental analysis (CHN), $C_{66}H_{84}N_{12}Cu_6S_3$, calculated (%): C 52.05, H 5.56, N 11.04; found (%): C 51.83, H 5.12, N 10.95.

Other inclusion complexes could be synthesized using same approach using different aromatic guest molecules.

Synthesis of 1⊃DCM. For comparison, the inclusion complex with non-aromatic guest, dichloromethane (DCM), was also prepared by solvent exchange reaction. The saturated solution (20 mL) of complex of **1⊃Py** in CH_2Cl_2 was mixed with methanol (10 mL). Then, the mixed solution was carried in a nitrogen stream for 30 min. The mixture (2 mL) was injected to the Pyrex glass tube and evaporated under darkness condition, obtaining colourless crystals 20 days later. IR spectrum (KBr pellets, cm^{-1}): 3429.81 (w), 3118.41 (b), 1662.35 (m), 1614.14 (m), 1453.11 (w), 1400.27 (vs), 1203.39 (w), 1148.06 (m), 1083.84 (m), 1055.26 (w), 790.26(w), 588.93 (w), 550.38 (w). ^{1}H NMR (400 MHz, CD_2Cl_2, 298 K): δ (ppm) 6.73 (s, 6H, CH_{thio}), 3.88 (s, 12H, CH_2), 2.58 (q, 24H, CH_2), 1.14 (t, 36H, CH_3). Elemental analysis (CHN), $C_{68}H_{88}N_{12}Cu_6S_3$, calculated (%): C 52.66, H 5.72, N 10.84; found (%): C 52.47, H 5.93, N 10.79.

Synthesis of 1⊃Ph-Me. The synthesis procedures were as same as the general method, the toluene (Ph) as aromatic guest was used instead of benzene. **1⊃Ph-Me** were obtained as light-brown block crystals (8.2 mg, yield 21.3 %, based on Cu). IR spectrum (KBr pellets, cm^{-1}): 3139.14 (b), 3078 (w), 1664.23 (m), 1616.50 (m), 1536.64 (w), 1503.79 (w), 1400.27 (s), 1303.67 (w), 1246.25 (w), 1205.36 (m), 1148.99 (w), 1083.61 (w), 1054.96 (s), 1027.69 (w), 975.40 (w), 917.68 (w), 790.80 (m), 724.69 (m), 688.31 (w), 512.12 (w). ^{1}H NMR (400 MHz, CD_2Cl_2, 298 K): δ (ppm) 7.18 (s, 4 H, Ph-H), 6.69 (s, 6H, CH_{thio}), 3.84 (s, 12H, CH_2), 2.54 (t, 24H, CH_2), 2.34 (s, 3H, Ph-Me), 1.10 (t, 36H, CH_3). Elemental analysis (CHN), $C_{67}H_{86}N_{12}Cu_6S_3$, calculated (%): C 52.36, H 5.64, N 10.94; found (%): C 52.13, H 5.84, N 10.78.

Synthesis of 1⊃Py. The synthesis procedures were as same as the general method, the pyridine (Py) as aromatic guest was used instead of benzene. **1⊃Py** were obtained as colorless block crystals (7.7 mg, yield 23.1 %, based on Cu). IR spectrum (KBr pellets, cm^{-1}): 3435.68 (b), 3057.75(w), 2964.27 (vs), 2925.47 (s), 2869.19 (w), 1574.14 (s), 1538.85 (m), 1505.71 (s), 1435.17 (s), 1368.86 (m), 1303.69 (w), 1246.60 (w), 1205.56 (m), 1151.28 (w), 1055.77 (s), 1027.51 (m), 972.97 (w), 917.91 (w), 860.58 (w), 792.87 (s), 750.78 (w), 723.66 (w), 709.77 (w), 694.87 (s), 669.16 (w), 587.80 (w). ^{1}H NMR (400 MHz, CD_2Cl_2, 298 K): δ (ppm) 7.63 (s, 2H, Py-H), 7.24 (s, 2H, Py-H), 6.62 (s, 6H, CH_{thio}), 3.78 (s, 12H, CH_2), 2.50 (br, 24H, CH_2), 1.18 (br, 36H, CH_3). Elemental analysis (CHN), $C_{65}H_{83}N_{13}Cu_6S_3$, calculated (%): C 51.23, H 5.49, N 11.95; found (%): C 51.42, H 5.54, N 11.67.

Synthesis of 1⊃Ph-NO_2. The synthesis procedures were as same as the general method, the

nitrobenzene(Ph-NO_2) as aromatic guest was used instead of benzene. **1⊃Ph-NO_2** were obtained as light-brown block crystals (15.8 mg, yield 39.6 %, based on Cu). IR spectrum (KBr pellets, cm^{-1}): 3435.34 (b), 3059.49 (w), 2961.99 (vs), 2925.16 (s), 2867.89 (s), 1618.51 (w), 1603.01 (w), 1523.51 (s), 1505.53 (s), 1435.81 (s), 1344.60 (m), 1314.38 (m), 1302.25 (w), 1245.51 (m), 1204.72 (m), 1147.56 (w), 1055.56 (s), 1023.82 (m), 791.51 (s), 766.56 (m), 700.29 (s). ^{1}H NMR (400 MHz, CD_2Cl_2, 298 K): δ (ppm) 8.20 (d, 2H, Ph-H), 7.70 (t, 1H, Ph-H), 7.55 (t, 2 H, Ph-H), 6.68 (s, 6H, CH_{thio}), 3.83 (s, 12H, CH_2), 2.53 (q, 24H, CH_2), 1.08 (t, 36H, CH_3). Elemental analysis (CHN), $C_{68}H_{77}N_{14}O_2Cu_6S_3$, calculated (%): C 51.05, H 4.85, N 12.26; found (%): C 50.87, H 4.69, N 12.51.

Synthesis of 1⊃OX. The synthesis procedures were as same as the general method, the *o*-xylene(OX) as aromatic guest was used instead of benzene. **1⊃Ph-NO_2** were obtained as light-brown block crystals (14.3 mg, yield 37.8 %, based on Cu). IR spectrum (KBr pellets, cm^{-1}): 3430.25 (b), 3054.86 (w), 2963.30 (vs), 2926.88 (s), 2869.72 (m), 1636.86 (w), 1537.37 (m), 1505.42 (s), 1436.05 (s), 1366.07 (s), 1316.64 (m), 1302.68 (m), 1245.43 (w), 1204.09 (m), 1148.83 (w), 1055.10 (s), 1023.80 (m), 975.04 (w), 915.75 (w), 791.69 (m), 767.44 (w), 742.59 (s), 656.09 (w), 575.82 (w), 514.25 (w). ^{1}H NMR (400 MHz, CD_2Cl_2, 298 K): δ (ppm) 7.09 (s, 4H, Ph-H), 6.69 (s, 6H, CH_{thio}), 3.84 (s, 12 H, CH_2), 2.55 (t, 24H, CH_2), 2.25 (s, 6H, -CH_3), 1.10 (t, 36H, CH_3). Elemental analysis (CHN), $C_{68}H_{88}N_{12}Cu_6S_3$, calculated (%): C 52.66, H 5.72, N 10.84; found (%): C 52.86, H 5.63, N 10.89.

Synthesis of 1⊃MX. The synthesis procedures were as same as the general method, the *m*-xylene(MX) as aromatic guest was used instead of benzene. **1⊃Ph-NO_2** were obtained as light-brown block crystals (13.7 mg, yield 35.4 %, based on Cu). IR spectrum (KBr pellets, cm^{-1}): 3429.81 (w), 3118.41 (b), 1662.35 (m), 1614.14 (m), 1453.11 (w), 1400.27 (vs), 1203.39 (w), 1148.06 (m), 1083.84 (m), 1055.26 (w), 790.26 (w), 588.93 (w), 550.38 (w). ^{1}H NMR (400 MHz, CD_2Cl_2, 298 K): δ (ppm) 7.65 (s, 1 H, Ph-H), 7.42 (s, 2H, Ph-H), 7.13 (s, 1H, Ph-H), 6.70 (s, 6H, CH_{thio}), 3.85 (s, 12H, CH_2), 2.54 (s, 24H, CH_2), 1.97 (s, 6H, -CH_3), 1.11 (s, 36H, CH_3). Elemental analysis (CHN), $C_{68}H_{88}N_{12}Cu_6S_3$, calculated (%): C 52.66, H 5.72, N 10.84; found (%): C 52.47, H 5.93, N 10.79.

Synthesis of 1⊃PX. The synthesis procedures were as same as the general method, the *m*-xylene(MX) as aromatic guest was used instead of benzene. **1⊃Ph-NO_2** were obtained as light-brown block crystals (7.2 mg, yield 18.6 %, based on Cu). IR spectrum (KBr pellets, cm^{-1}): 3420.56 (b), 3330.25 (w), 3054.86 (w), 2963.30 (vs), 2943.18 (w), 2921.38 (s), 2867.78 (m), 1636.86 (w), 1537.37 (w), 1505.42 (s), 1436.05 (s), 1366.07 (s),1316.64 (m), 1302.68 (m), 1245.43 (w), 1204.09 (m), 1148.83 (w), 1055.10 (s), 1025.50(m), 975.04 (w), 915.75 (w), 791.69 (m), 767.44 (w), 742.59 (s), 656.09 (w), 575.82 (w), 556.23 (w), 532.45 (w). ^{1}H NMR (400 MHz, CD_2Cl_2, 298 K): δ (ppm) 7.05 (s, 4 H, Ph-H), 6.69 (s, 6H, CH_{thio}), 3.84 (s, 12H, CH_2), 2.55 (t, 24H, CH_2), 2.28 (s, 6H, -CH_3), 1.10 (t, 36H, CH_3). Elemental analysis (CHN), $C_{68}H_{88}N_{12}Cu_6S_3$, calculated (%): C 52.66, H 5.72, N 10.84; found (%): C 52.79, H 5.64, N 10.68.

2. Crystal data

2.1. Crystal structure determination

Suitable crystal of the inclusion complexes was mounted with glue at the end of a glass fiber. Data collection was performed with an Oxford Diffraction Gemini E instrument (Cu X-ray source, Kα, λ = 1.54056 Å; Mo X-ray source, Kα, λ = 0.71073 Å) equipped with a graphite monochromator and ATLAS CCD detector (CrysAlis CCD, Oxford Diffraction Ltd.) and a XtaLab PRO MM007HF DW Diffractometer System equipped with a MicroMax-007DW MicroFocus X-ray generator and Pilatus200K silicon diarray detector (Rigaku, Japan). The structure was solved by direct methods (SHELXL-2014 and Olex2) and refined by full-matrix least-squares refinements based on F^2. Anisotropic thermal parameters were applied to all non-hydrogen atoms. The hydrogen atoms were generated geometrically. The treatment for the disordered guest molecules in the cavities of all complexes involved the use of the SQUEEZE program of PLATON. Crystal data and structure refinement are summarized in Table S1-S4. CCDC Nos. 1963722, and 1963726-1963732.

Table S1. Crystal data and structure refinements for inclusion complexes.

Parameter	1⊃DCM	1⊃Py	1⊃Ph	1⊃Ph-Me
Formula	$C_{60}H_{78}N_{12}Cu_6S_3$	$C_{65}H_{83}N_{13}Cu_6S_3$	$C_{66}H_{84}N_{12}Cu_6S_3$	$C_{67}H_{86}N_{12}Cu_6S_3$
F.W.	1529.76	1523.86	1522.87	1536.90
Crystal system	monoclinic	monoclinic	monoclinic	monoclinic
Space group	$P2_1/c$	$P2_1/c$	$P2_1/c$	$P2_1/c$
Temperature (K)	100(2)	298(2)	298(2)	298(2)
a (Å)	28.6943(2)	19.5415(9)	19.5811(9)	19.6504(6)
b (Å)	24.1131(2)	24.1626(11)	24.1470(10)	24.2067(7)
c (Å)	19.8986(2)	15.6523(8)	15.6493(11)	15.6844(5)
α (°)	90	90	90	90
β (°)	107.5100(10)	110.968(5)	110.884(7)	110.567(4)
γ (°)	90	90	90	90
V (Å^3)	13130.1(2)	6901.2(6)	6913.3(6)	6985.1(4)
Z	2	4	4	4
D_c (g·cm^{-3})	2.856	1.467	1.463	1.461
μ (mm^{-1})	15.257	3.239	3.228	3.200
Reflns collected	127232	29961	24417	48884
Unique reflns	27417	14333	14192	14746
R_{int}	0.07	0.0369	0.0571	0.0579
GOF on F^2	1.025	1.008	1.014	2.905
R_1[I≥2σ(I)] [a]	0.0855	0.1392	0.1547	0.2052
wR_2[I≥2σ(I)] [b]	0.2289	0.3776	0.3889	0.5118
R_1[all data]	0.0932	0.1670	0.1860	0.2287
wR_2[all data]	0.2340	0.4024	0.4165	0.5326
CCDC number	1963732	1963722	1963726	1963727

[a] $R_1 = \Sigma(||F_0| - |F_c||)/\Sigma|F_0|$; [b] $wR_2 = [\Sigma w(F_0^2 - F_c^2)^2/\Sigma w(F_0^2)^2]^{1/2}$

Table S2. Crystal data and structure refinements for Complexes.

Parameter	1⊃Ph-NO_2	1⊃MX	1⊃OX	1⊃PX
Formula	$C_{68}H_{77}N_{14}O_2Cu_6S_3$	$C_{70}H_{86}N_{13}Cu_6S_3$	$C_{68}H_{89}N_{13}Cu_6S_3$	$C_{68}H_{88}N_{12}Cu_6S_3$
F.W.	1599.8	1586.94	1560.75	1550.92
Crystal system	triclinic	triclinic	triclinic	monoclinic
Space group	*P*-1	*P*-1	*P*-1	$P2_1/c$
Temperature (K)	298(2)	298(2)	298(2)	298(2)
a (Å)	10.3507(3)	10.3000(10)	10.4866(3)	14.5207(2)
b (Å)	14.9589 (5)	14.9840(3)	14.9130(5)	23.6798(5)
c (Å)	24.1232(8)	23.8025(4)	23.7782(9)	20.9116(4)
α (°)	84.466(3)	83.2120(10)	84.4830(10)	90
β (°)	80.595(3)	80.006(2)	86.955(3)	102.454(2)
γ (°)	77.955(3)	77.041(2)	78.425(3)	90
V ($Å^3$)	3596.3(2)	3506(341)	3623.9(2)	7021.2(2)
Z	2	1	2	4
D_c ($g\cdot cm^{-3}$)	1.477	1.503	1.455	1.467
μ (mm^{-1})	3.166	1.927	1.865	3.189
Reflns collected	26198	38520	24037	52682
Unique reflns	14887	13638	13427	14813
R_{int}	0.0263	0.0510	0.0280	0.0323
GOOF on F^2	0.993	1.026	1.111	1.025
$R_1[I\geq 2\sigma(I)]^a$	0.0620	0.0692	0.0682	0.0520
$wR_2[I\geq 2\sigma(I)]^b$	0.1964	0.1927	0.1934	0.1481
R_1[all data]	0.0797	0.0808	0.0836	0.0743
wR_2[all data]	0.2237	0.2027	0.2151	0.1692
CCDC number	1963730	1963731	1963729	1963728

[a] $R_1 = \Sigma(||F_0| - |F_c||)/\Sigma|F_0|$; [b] $wR_2 = [\Sigma w(F_0^2 - F_c^2)^2/\Sigma w(F_0^2)^2]^{1/2}$

Table S3. Selected bond lengths (Å) and bond angles (°) of complexes.

1⊃Py			
Cu(1)-N(1)	1.843(8)	Cu(1)-N(9)	1.862(9)
Cu(1)-Cu(2)#1	2.969(2)	Cu(2)-N(5)	1.851(9)
Cu(2)-N(2)	1.863(7)	Cu(2)-Cu(1)#1	2.969(2)
Cu(3)-N(10)	1.840(9)	Cu(3)-N(6)	1.848(10)
Cu(4)-N(12)	1.864(12)	Cu(4)-N(3)	1.866(11)
Cu(5)-N(7)	1.827(18)	Cu(5)-N(4)	1.854(15)
Cu(6)-N(8)	1.771(18)	Cu(6)-N(11)	1.871(12)
1⊃Ph			
Cu(1)-N(1)	1.855(9)	Cu(1)-N(9)	1.860(10)
Cu(1)-Cu(2)#1	2.970(3)	Cu(2)-N(5)	1.859(10)
Cu(2)-N(2)	1.863(8)	Cu(2)-Cu(1)#1	2.970(3)
Cu(3)-N(10)	1.843(10)	Cu(3)-N(6)	1.857(11)
Cu(4)-N(3)	1.854(12)	Cu(4)-N(12)	1.871(13)
Cu(5)-N(7)	1.823(17)	Cu(5)-N(4)	1.846(16)
Cu(6)-N(8)	1.74(2)	Cu(6)-N(11)	1.870(13)
N(1)-Cu(1)-N(9)	172.6(4)	N(1)-Cu(1)-Cu(2)#1	95.6(3)
N(5)-Cu(2)-N(2)	173.5(5)	N(9)-Cu(1)-Cu(2)#1	91.6(3)
N(10)-Cu(3)-N(6)	173.5(5)	N(5)-Cu(2)-Cu(1)#1	94.6(4)
N(3)-Cu(4)-N(12)	174.2(7)	N(2)-Cu(2)-Cu(1)#1	91.8(3)
N(7)-Cu(5)-N(4)	174.5(6)	N(8)-Cu(6)-N(11)	173.9(6)
N(2)-N(1)-Cu(1)	120.0(6)	C(3)-N(1)-Cu(1)	129.8(7)
N(1)-N(2)-Cu(2)	120.3(6)	C(5)-N(2)-Cu(2)	130.7(8)
1⊃Ph-Me			
Cu(1)-N(1)	1.798(7)	Cu(1)-N(10)	1.819(10)
Cu(2)-N(5)	1.737(11)	Cu(2)-N(2)	1.851(9)
Cu(3)-N(6)	1.719(11)	Cu(3)-N(9)	1.824(10)
Cu(4)-N(3)	1.807(5)	Cu(4)-N(12)	1.852(7)

Cu(4)-Cu(5)#1	2.982(3)	Cu(5)-N(7)	1.811(6)
Cu(5)-N(4)	1.816(5)	Cu(5)-Cu(4)#1	2.982(3)
Cu(6)-N(8)	1.823(7)	Cu(6)-N(11)	1.847(8)
N(1)-Cu(1)-N(10)	170.5(6)	N(5)-Cu(2)-N(2)	174.9(5)
N(6)-Cu(3)-N(9)	175.2(5)	N(3)-Cu(4)-N(12)	173.9(4)
N(7)-Cu(5)-N(4)	174.6(4)	N(3)-Cu(4)-Cu(5)#1	93.6(2)
N(8)-Cu(6)-N(11)	172.2(4)	N(12)-Cu(4)-Cu(5)#1	92.2(3)
N(2)-N(1)-Cu(1)	115.3(8)	N(7)-Cu(5)-Cu(4)#1	95.8(3)
C(3)-N(1)-Cu(1)	136.6(8)	N(4)-Cu(5)-Cu(4)#1	89.6(3)
N(1)-N(2)-Cu(2)	119.8(7)	C(5)-N(2)-Cu(2)	132.0(7)

Symmetry Code: #1 -x+1,-y+1,-z+1

		1⊃PX	
Cu(1)-N(10)	1.862(3)	Cu(1)-N(1)	1.863(3)
Cu(2)-N(2)	1.860(3)	Cu(2)-N(5)	1.865(3)
Cu(3)-N(9)	1.858(3)	Cu(3)-N(6)	1.861(3)
Cu(4)-N(12)	1.861(4)	Cu(4)-N(3)	1.862(4)
Cu(5)-N(4)	1.854(3)	Cu(5)-N(7)	1.855(3)
Cu(6)-N(11)	1.855(4)	Cu(6)-N(8)	1.861(4)
N(10)-Cu(1)-N(1)	172.27(15)	N(2)-Cu(2)-N(5)	177.21(15)
N(9)-Cu(3)-N(6)	178.57(15)	N(12)-Cu(4)-N(3)	175.61(16)
N(4)-Cu(5)-N(7)	176.83(18)	N(11)-Cu(6)-N(8)	175.69(16)
C(3)-N(1)-Cu(1)	131.9(3)	N(2)-N(1)-Cu(1)	118.5(2)
C(5)-N(2)-Cu(2)	133.0(3)	N(1)-N(2)-Cu(2)	118.9(2)
N(4)-N(3)-Cu(4)	117.4(3)	N(3)-N(4)-Cu(5)	119.5(3)
N(5)-N(6)-Cu(3)	117.6(2)	N(8)-N(7)-Cu(5)	119.8(3)
		1⊃OX	
Cu(1)-N(11)	1.861(11)	Cu(1)-N(10)	1.863(5)
Cu(2)-N(2)	1.860(3)	Cu(2)-N(3)	1.859(4)

Cu(3)-N(4)	1.862(10)	Cu(3)-N(5)	1.867(6)
Cu(4)-N(12)	1.847(5)	Cu(4)-N(7)	1.854(4)
Cu(5)-N(9)	1.857(4)	Cu(5)-N(8)	1.865(7)
Cu(5)-Cu(6)#1	3.0(2)	Cu(6)-N(6)	1.858(4)
Cu(6)-N(1)	1.868(6)	Cu(6)-Cu(5)#2	3.0(2)
N(11)-Cu(1)-N(10)	174.2(5)	N(2)-Cu(2)-N(3)	177.0(2)
N(4)-Cu(3)-N(5)	175.3(4)	N(12)-Cu(4)-N(7)	177.46(17)
N(9)-Cu(5)-N(8)	171.3(8)	N(9)-Cu(5)-Cu(6)#1	85.2(3)
N(6)-Cu(6)-N(1)	172.9(7)	N(8)-Cu(5)-Cu(6)#1	103.2(10)
N(2)-N(1)-Cu(6)	118.5(4)	N(6)-Cu(6)-Cu(5)#2	112(2)
C(5)-N(2)-Cu(2)	131.4(8)	N(1)-Cu(6)-Cu(5)#2	75(3)
1⊃Ph-NO_2			
Cu(1)-N(5)	1.862(4)	Cu(2)-N(6)	1.856(4)
Cu(2)-N(9)	1.857(3)	Cu(3)-N(2)	1.854(4)
Cu(3)-N(10)	1.856(4)	Cu(4)-N(3)	1.844(4)
Cu(4)-N(7)	1.847(4)	Cu(5)-N(11)	1.852(4)
Cu(5)-N(8)	1.858(4)	Cu(6)-N(12)	1.857(4)
Cu(6)-N(4)	1.866(4)	Cu(1)-N(1)	1.865(4)
N(5)-Cu(1)-N(1)	171.18(17)	N(6)-Cu(2)-N(9)	175.1(2)
N(2)-Cu(3)-N(10)	176.42(19)	N(3)-Cu(4)-N(7)	177.13(18)
N(11)-Cu(5)-N(8)	173.90(18)	N(12)-Cu(6)-N(4)	172.59(17)
C(12)-S(1)-C(9)	94.1(2)	C(29)-S(2)-C(32)	92.7(3)
C(52)-S(3)-C(49)	93.1(2)	C(5)-N(1)-Cu(1)	132.3(3)
N(2)-N(1)-Cu(1)	118.8(3)	N(4)-N(3)-Cu(4)	120.3(3)
1⊃MX			
Cu(1)-N(2)	1.864(5)	Cu(1)-N(3)	1.871(6)
Cu(2)-N(5)	1.851(5)	Cu(2)-N(4)	1.854(4)
Cu(3)-N(6)	1.867(14)	Cu(3)-N(1)	1.869(7)
Cu(4)-N(9)	1.856(5)	Cu(4)-N(8)	1.855(4)

Cu(5)-N(11)	1.859(4)	Cu(5)-N(10)	1.871(7)
Cu(6)-N(7)	1.866(15)	Cu(6)-N(12)	1.872(14)
N(2)-Cu(1)-N(3)	173.4(6)	N(5)-Cu(2)-N(4)	177.54(18)
N(6)-Cu(3)-N(1)	175.0(4)	N(9)-Cu(4)-N(8)	175.9(4)
N(11)-Cu(5)-N(10)	172.6(7)	N(7)-Cu(6)-N(12)	177.4(2)
C(3)-N(1)-Cu(3)	130.4(5)	N(2)-N(1)-Cu(3)	120.8(4)
N(6)-N(5)-Cu(2)	119.1(6)	N(5)-N(6)-Cu(3)	118.0(4)

Table S4. The selected structure parameter of the crystal

Complexes[a]	Intratrimer Cu···Cu (Å)	Intertrimer[b] Cu···Cu (Å)	Cu_3···Cu_3 (Å)	Cu_3···C_6 (arene) (Å)	Intermolecular Cu···Cu (Å)	Guest Volume (Å^3)	Host Volume (Å^3)
1⊃DCM	3.163-3.248	6.734-7.098	6.923	–	2.796-3.051	43.7	218.18
1⊃Py	3.153-3.200	6.889-6.962	6.933	3.462/3.470	2.96	79.40	240.85
1⊃Ph	3.145-3.201	6.901-6.964	6.936	3.473/3.466	2.97	84.46	243.32
1⊃Ph-Me	3.108-3.185	6.964-7.012	6.988	[d]3.98/3.98	2.982/3.454	102.55	267.01
1⊃Ph-NO_2	3.171-3.206	6.794-6.867	6.835	3.415/3.442	3.139	108.03	266.49
1⊃OX	3.162-3.206	6.904-7.022	6.953	3.623/3.548	3.042	119.87	262.30
1⊃MX	3.098-3.245	6.726-3.866	6.791	3.555/3.416	3.183	120.52	261.44
1⊃PX	3.154-3.241	6.456-7.074	6.811	3.502/3.501	3.793/3.925	120.65	256.50

a: The X-ray data of all complexes were determined at 298 K; b: The Cu···Cu distance between two cyclic trinuclear units in each cage.

2.2. Illustration of the single complex molecule

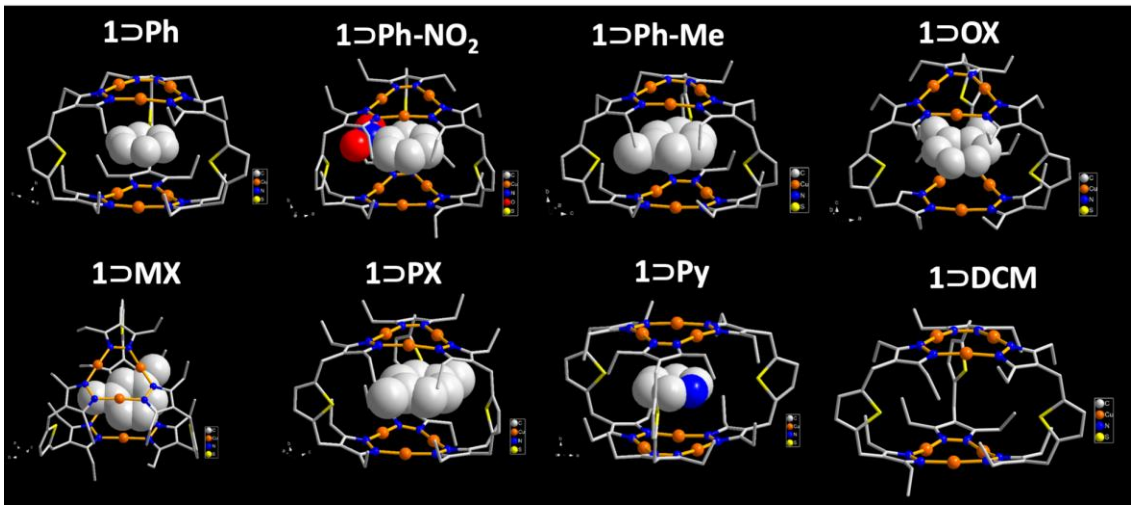

Figure S3. X-ray crystal structure of inclusion complexes (only the cage host unit in each complex is shown). Cu and N atoms are represented by orange, and blue spheres, respectively, whereas the frames are depicted as sticks (C black, S yellow), and the guests are depicted as space-filling (C gray, N blue, I pink, O red, Br brown, Cl green).

2.3. Crystal images of the crystal sample

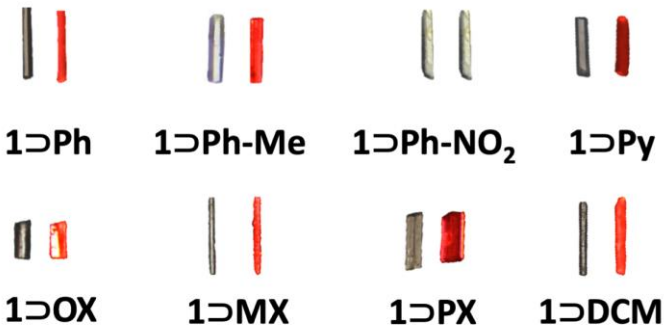

Figure S4. Images of the inclusion crystal amplified 40 times by microscope under natural light (left) and the excitation of 365 nm (right).

3. Additional Characterization Section

3.1. the ratio of host and guest and the ^{1}H NMR spectra of complexes

Table S5. the ratio of host and guest was detected by ^{1}H NMR.

Complex	Host : Guest
1⊃Ph	1 : 1
1⊃Ph-Me	1 : 1
1⊃OX	1 : 1
1⊃MX	1 : 1
1⊃PX	1 : 1
1⊃Ph-NO$_2$	1 : 1
1⊃Py	1 : 1

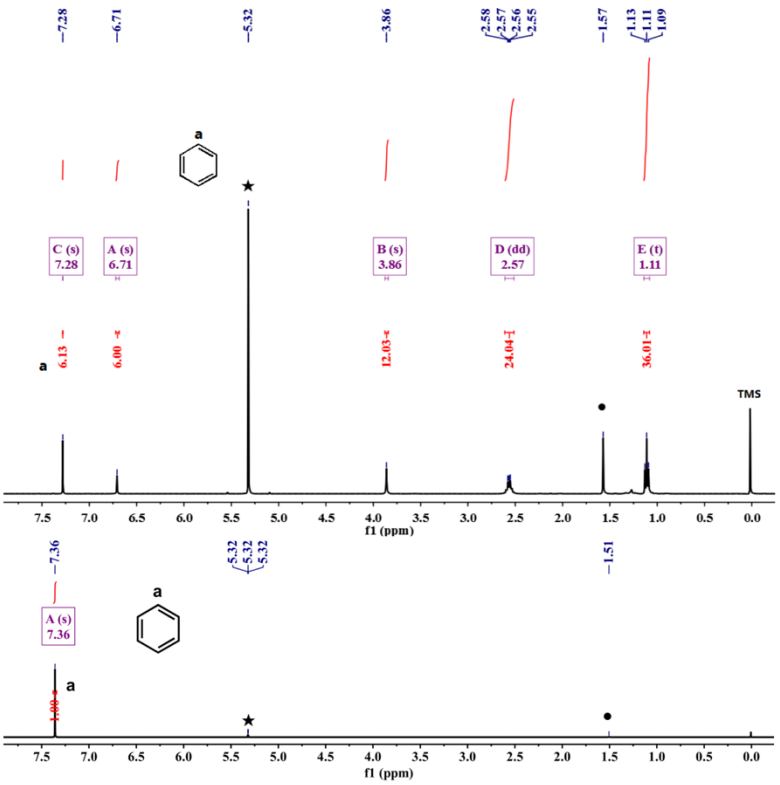

Figure S5. ^{1}H NMR (400 MHz, CD_2Cl_2, 298 K) spectra of **1⊃Ph** (top) and guest **Ph** (bottom)

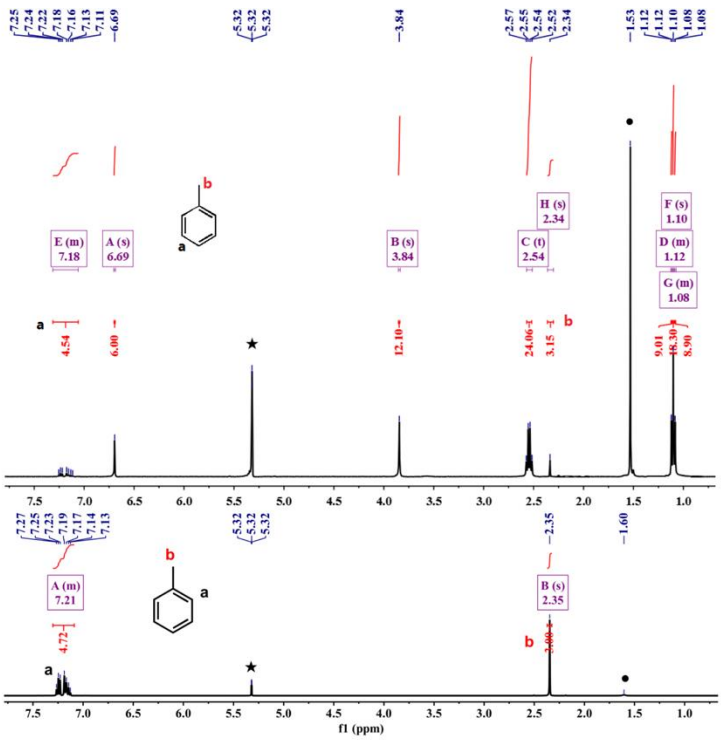

Figure S6. ^{1}H NMR (400 MHz, CD_2Cl_2, 298 K) spectra of **1⊃Ph-Me** (top) and guest **Ph-Me** (bottom)

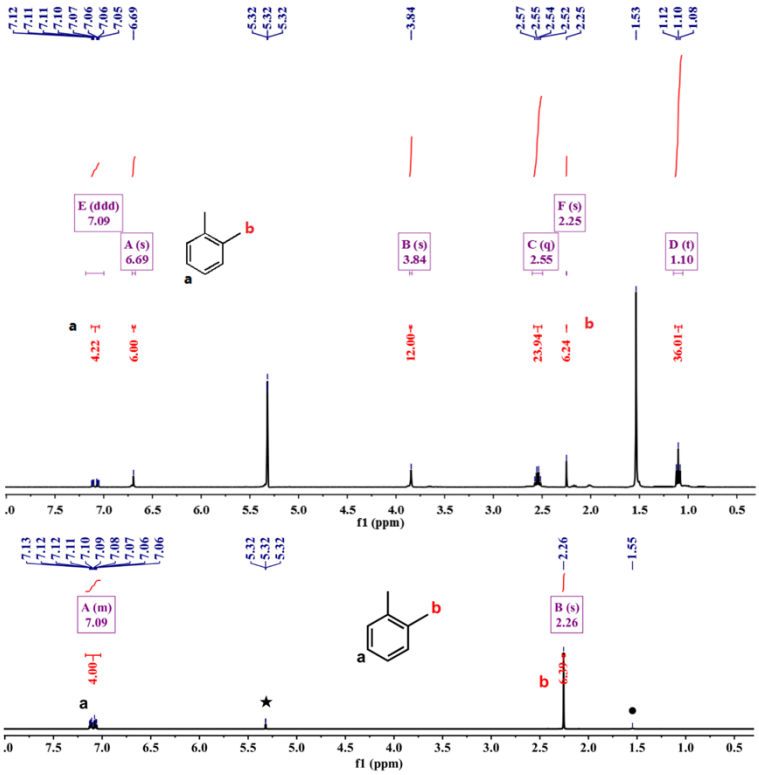

Figure S7. ^{1}H NMR (400 MHz, CD_2Cl_2, 298 K) spectra of **1⊃OX** (top) and guest **OX** (bottom)

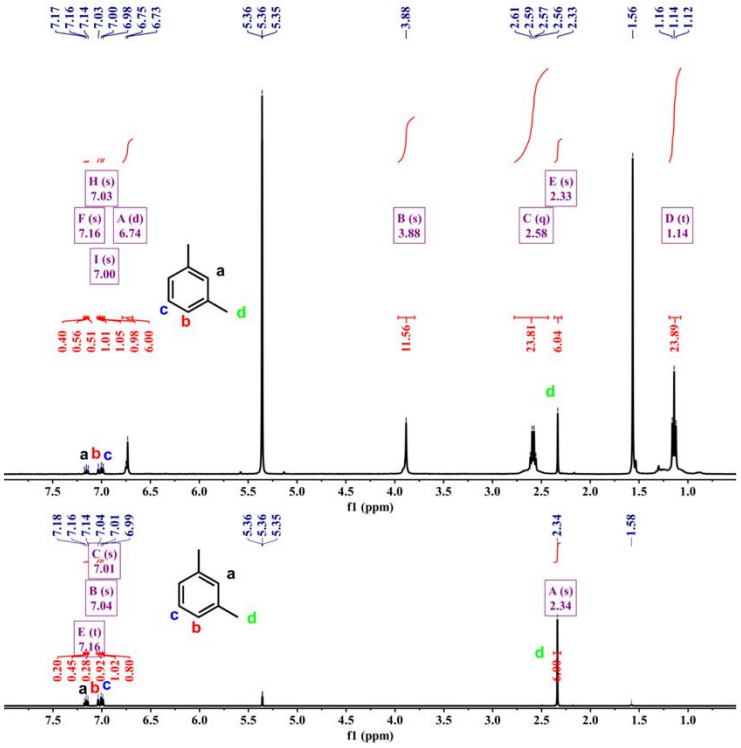

Figure S8. ^{1}H NMR (400 MHz, CD_2Cl_2, 298 K) spectra of **1⊃MX** (top) and guest **MX** (bottom)

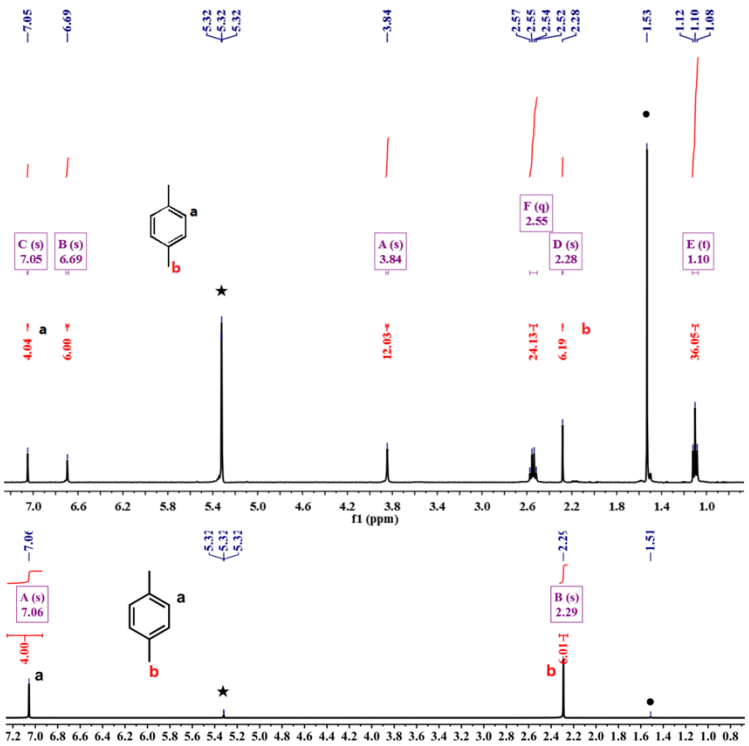

Figure S9. ^{1}H NMR (400 MHz, CD_2Cl_2, 298 K) spectra of **1⊃PX** (top) and guest **PX** (bottom)

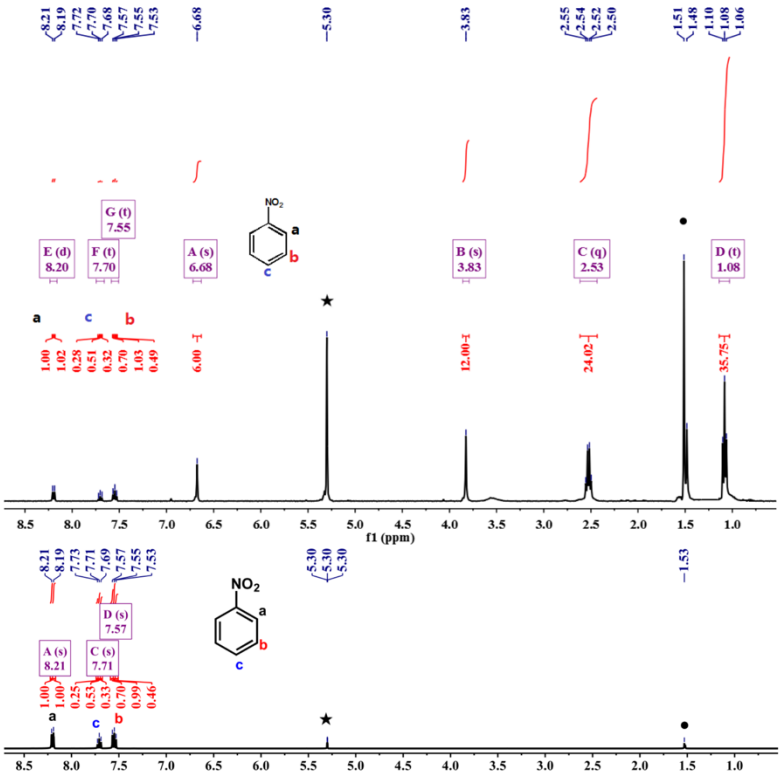

Figure S10. ^{1}H NMR (400 MHz, CD_2Cl_2, 298 K) spectra of **1⊃Ph-NO₂** (top) and guest **1⊃Ph-NO₂** (bottom)

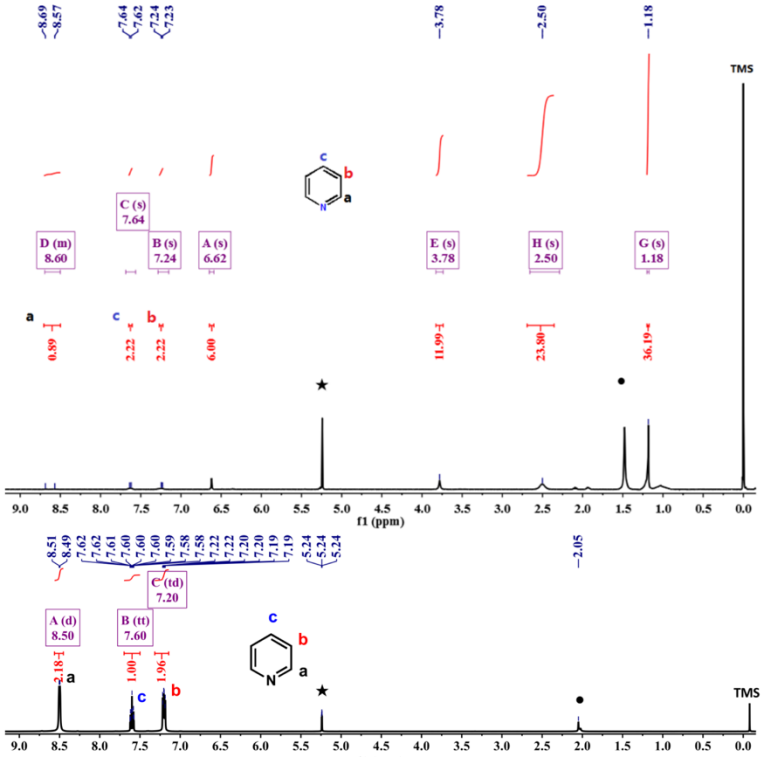

Figure S11. ^{1}H NMR (400 MHz, CD_2Cl_2, 298 K) spectra of **1⊃Py** (top) and guest **1⊃Py** (bottom)

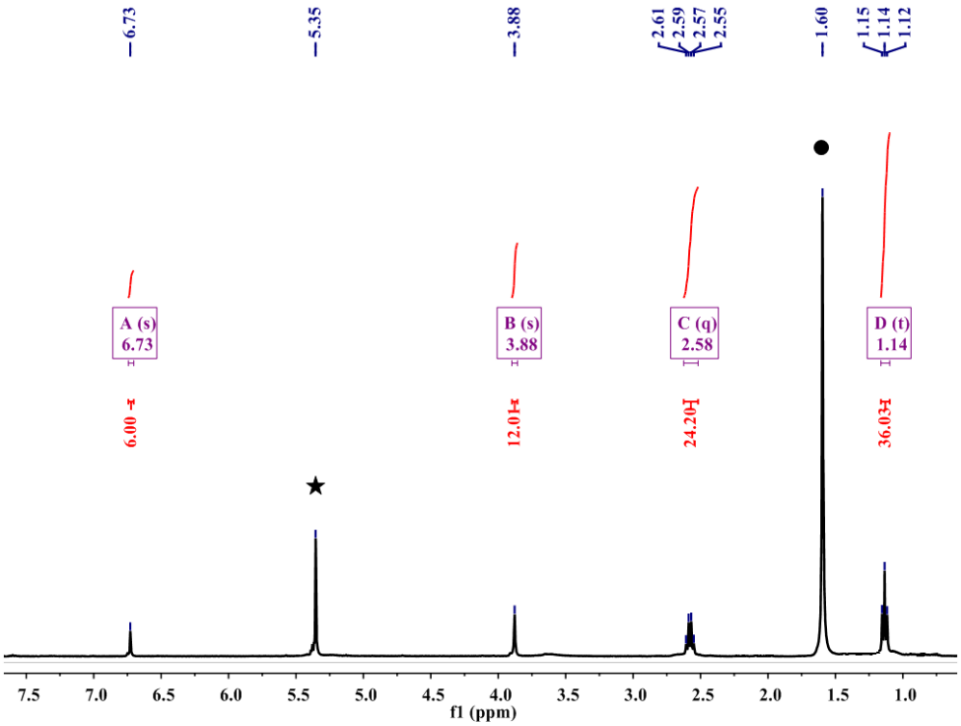

Figure S12. ^{1}H NMR (400 MHz, CD_2Cl_2, 298 K) spectra of **1⊃DCM**

3.2. TGA analysis

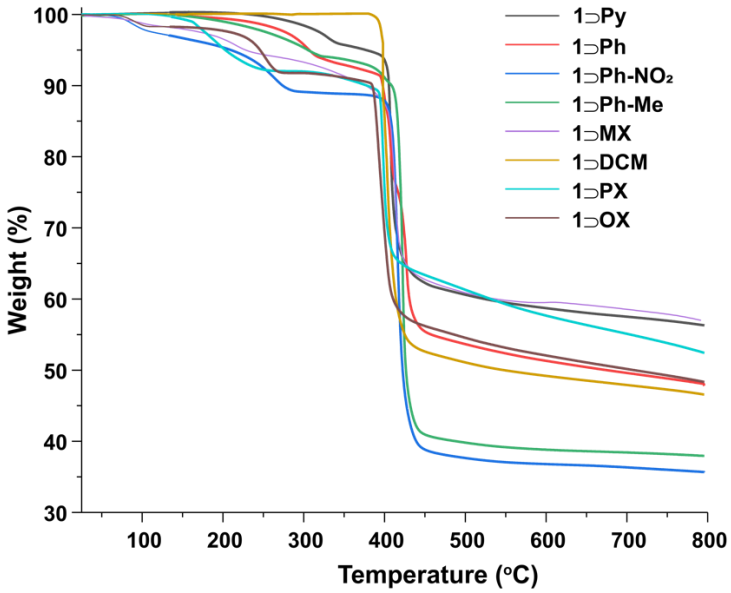

Figure S13. The TGA analysis spectra of inclusion complexes. All complexes decomposed at 390 °C. Then the TGA curves also demonstrate the temperature of escaping with the guests are ranging from 200 to 280°C far higher than the boiling point of guest molecules, indicating the guests are strongly holed within the cavity of Cu_6L_3 cage.

3.3. IR spectra of inclusion complexes

All inclusion complexes were also characterized by IR spectra, showing a strong absorption peaks at around 3100 cm^{-1} (Figure S14), attributed to the thienyl group (C-H_s). In addition, there exists a strong absorption peak at around 1400 and 1500 cm^{-1} corresponding to the N=N bonds stretching in the ligands. New absorption peaks appeared at 1000 cm^{-1} and 500-700 cm^{-1} are assigned to the vibration of the guests (ν_{C-X} or C-H_s). Importantly, the vanishing of N-H bond stretching indicting the deprotonation during the formation of coordination bond between Cu(I) ions and N atom.

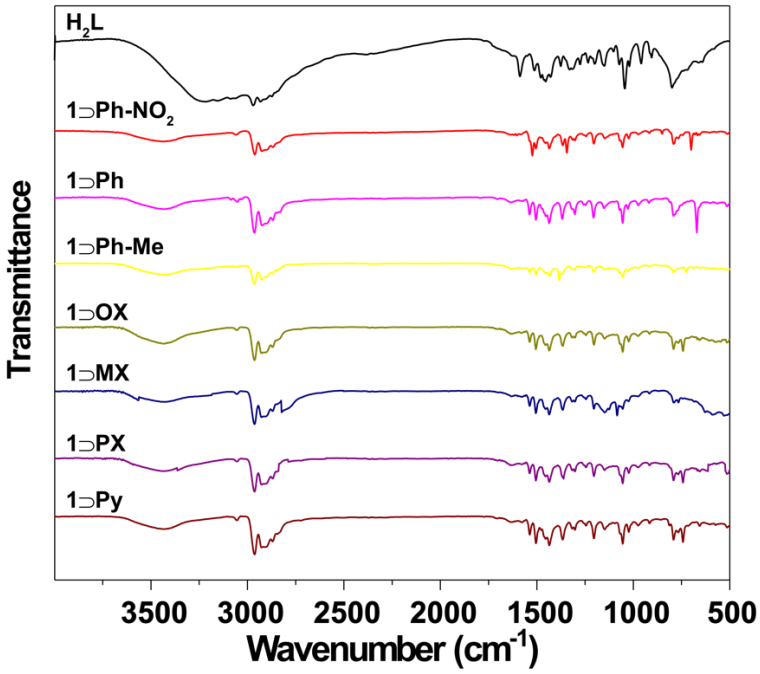

Figure S14. IR spectra of all inclusion complexes.

3.4. Powder X-ray diffraction of inclusion complexes

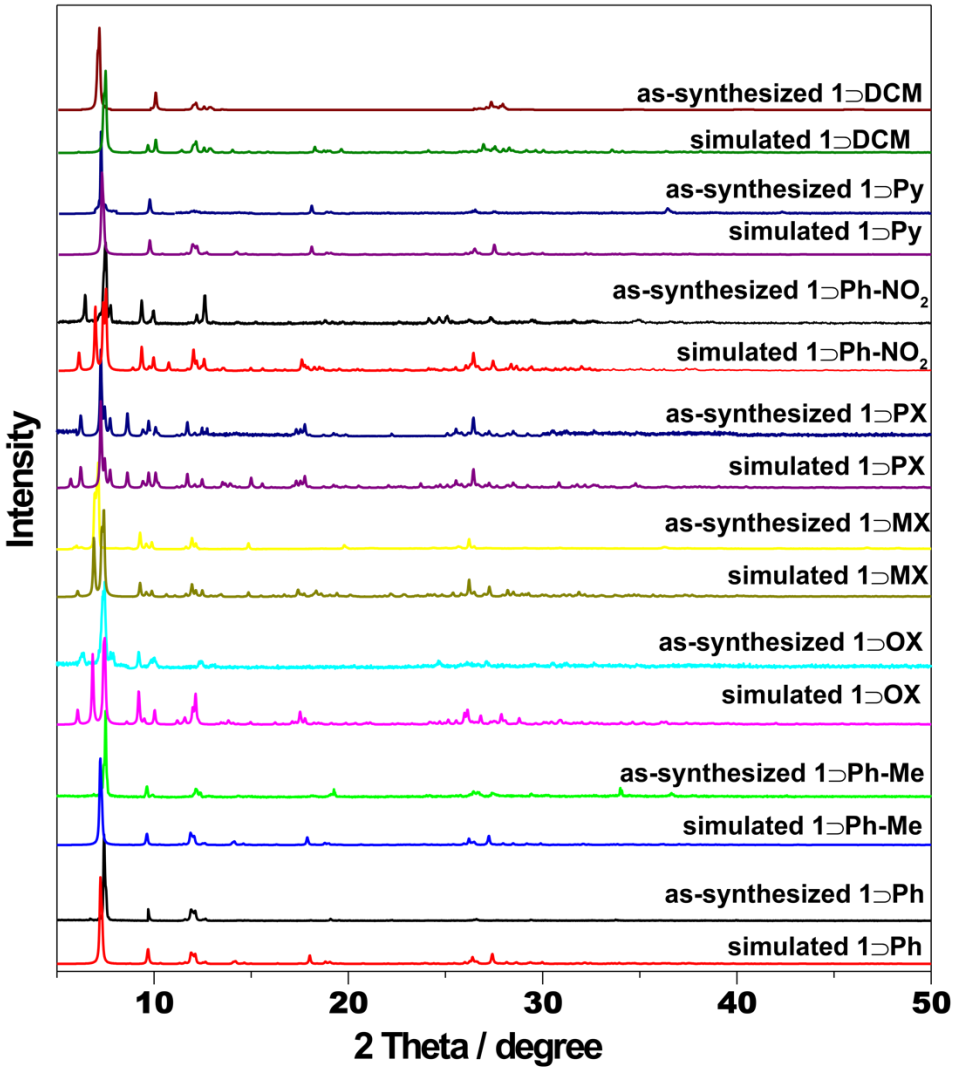

Figure S15. The comparison of as-synthesized and simulated powder X-ray diffraction spectra of inclusion complexes.

4. Photoluminescence Measurement Section

4.1. Solid-state UV-vis spectra of the complexes

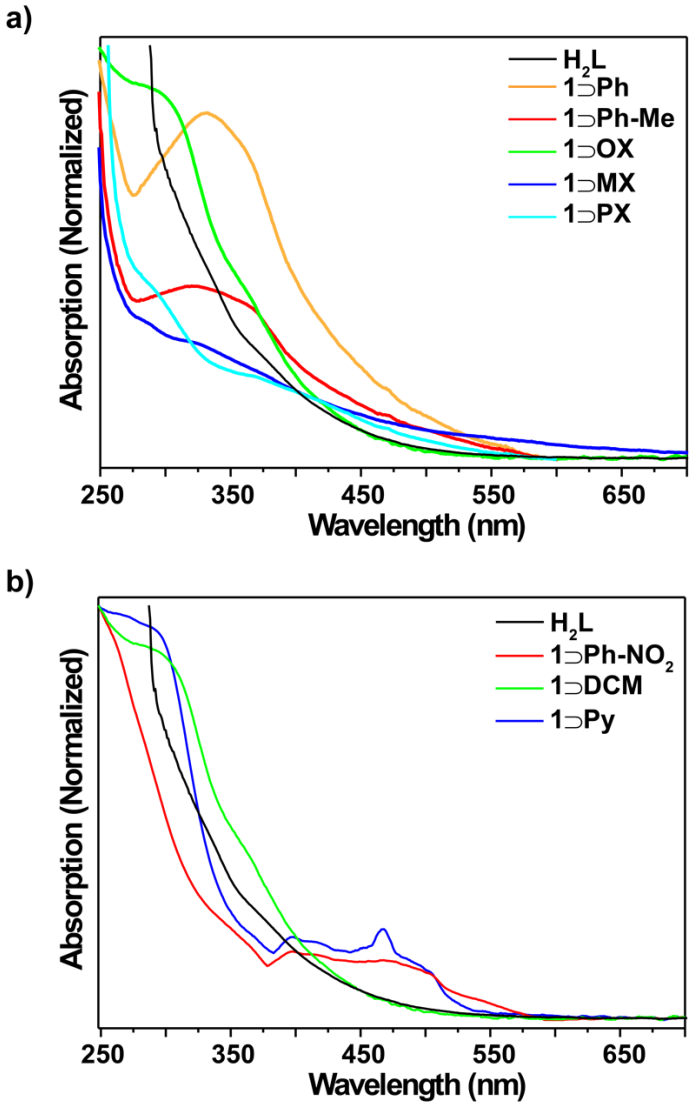

Figure S16. Normalized solid-state UV-vis spectra of (a) **H_2L**, **1⊃Ph**, **1⊃Ph-Me**, **1⊃OX**, **1⊃MX**, and **1⊃PX**; (b) **H_2L**, **1⊃Py**, **1⊃Ph-NO_2**, and **1⊃DCM**. The sample were measured under the same concentration.

4.2. Solution-state UV-vis spectra of inclusion complexes

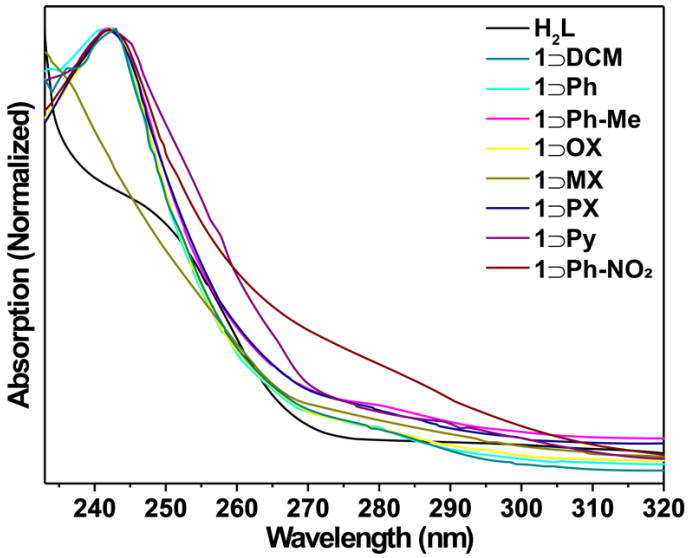

Figure S17. Normalized solution (DCM) UV-vis spectra of inclusion complexes. The sample were measured under the same concentration.

4.3. The emission spectra of inclusion complexes

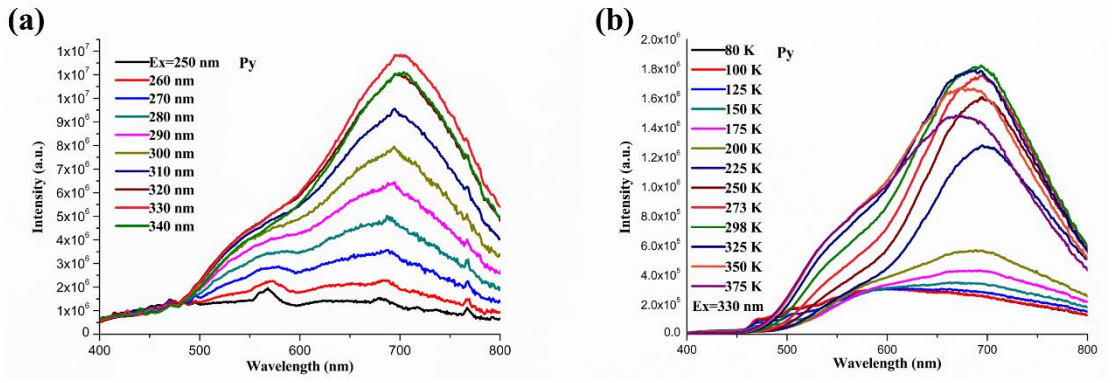

Figure S18. Excitation-energy-varied (a) and temperature-varied (b) emission spectra of **1⊃Py** (Ex=330 nm).

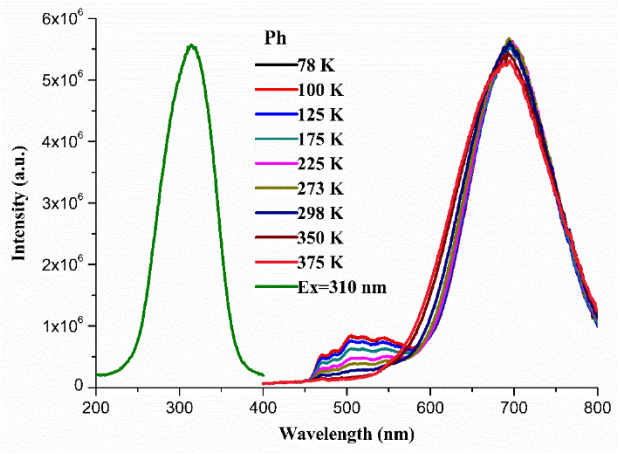

Figure S19. Temperature-varied emission spectra of **1⊃Ph** (Ex=310 nm).

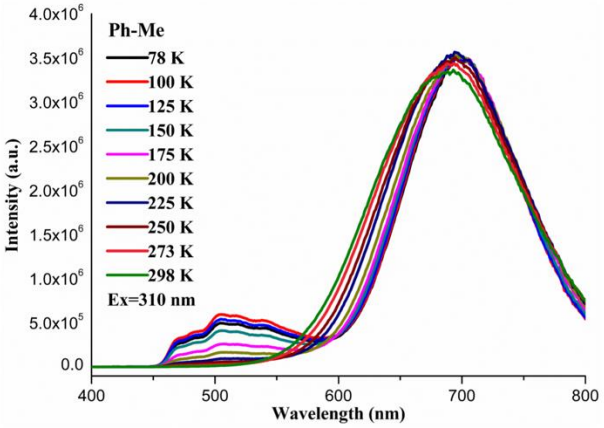

Figure S20. Temperature-varied emission spectra of **1⊃Ph-Me**, (b) (Ex=310 nm).

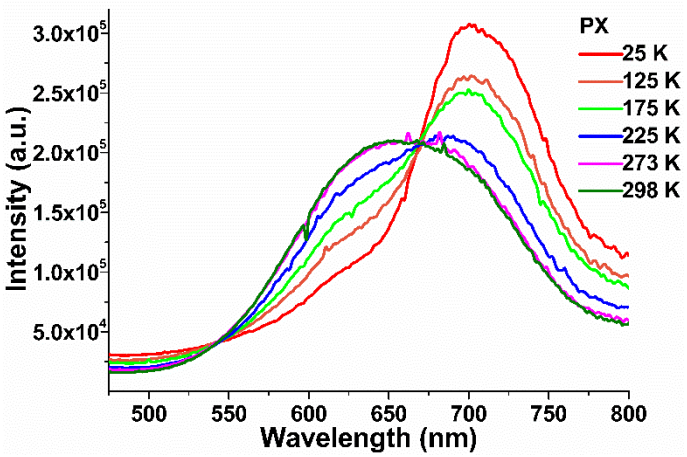

Figure S21. Temperature-varied emission spectrum of **1⊃PX** (Ex=320 nm).

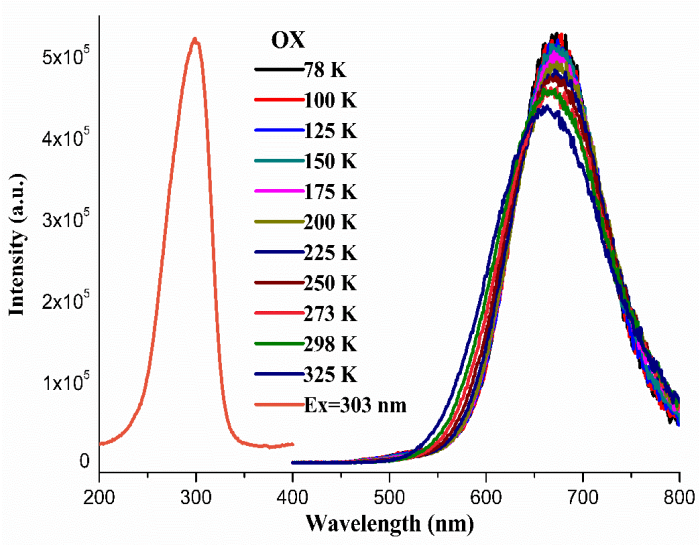

Figure S22. Temperature-varied emission spectra of **1⊃OX** (Ex=303 nm)

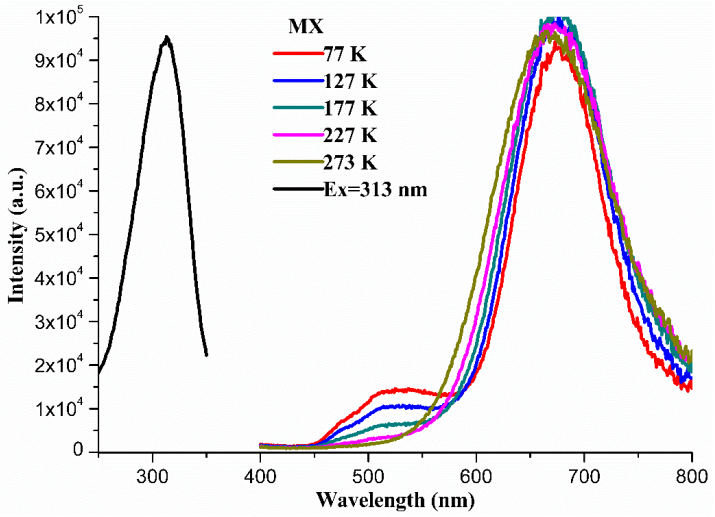

Figure S23. Temperature-varied emission spectra of **1⊃PX** (Ex=313 nm).

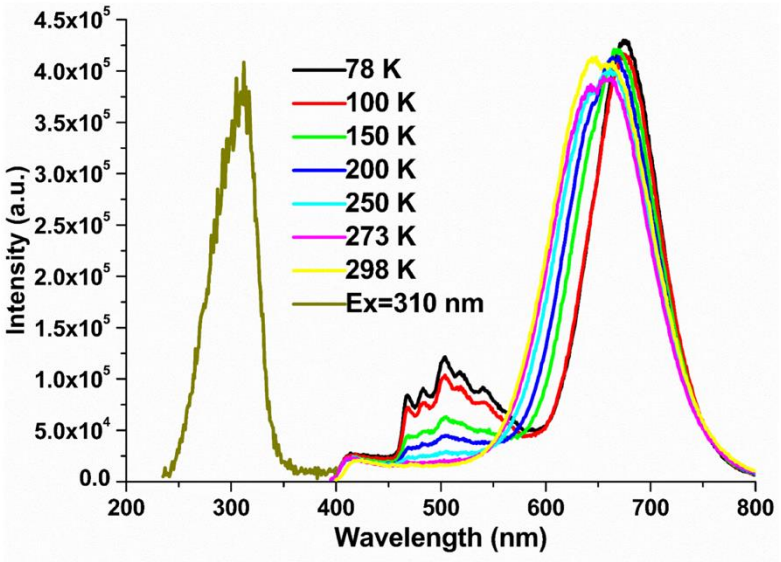

Figure S24. Temperature-varied emission spectra of **1⊃DCM** (Ex=310 nm)

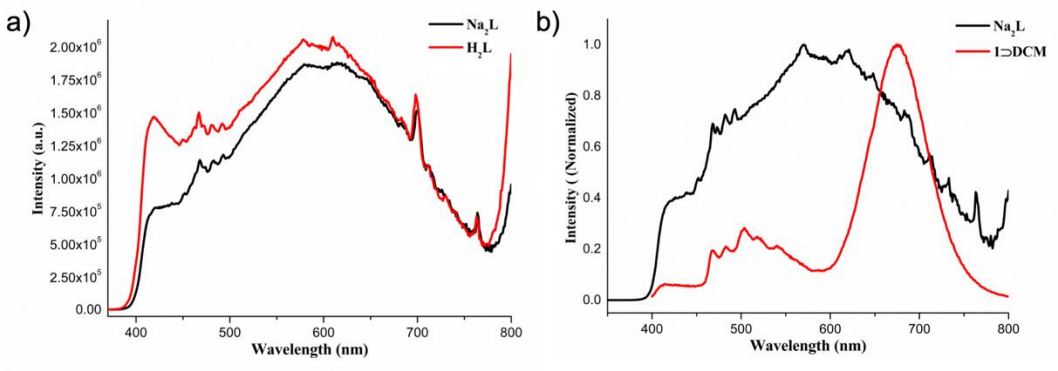

Figure S25. Emission spectra of a) **Na_2L** (black line) and **H_2L** (red line) and b) **Na_2L** (black line) and **1⊃DCM** (red line). (The deprotonated ligand, **Na_2L** can be obtained by deprotonation of ligand **H_2L** with NaH in the THF solution.)

4.5. Lifetime data of complexes

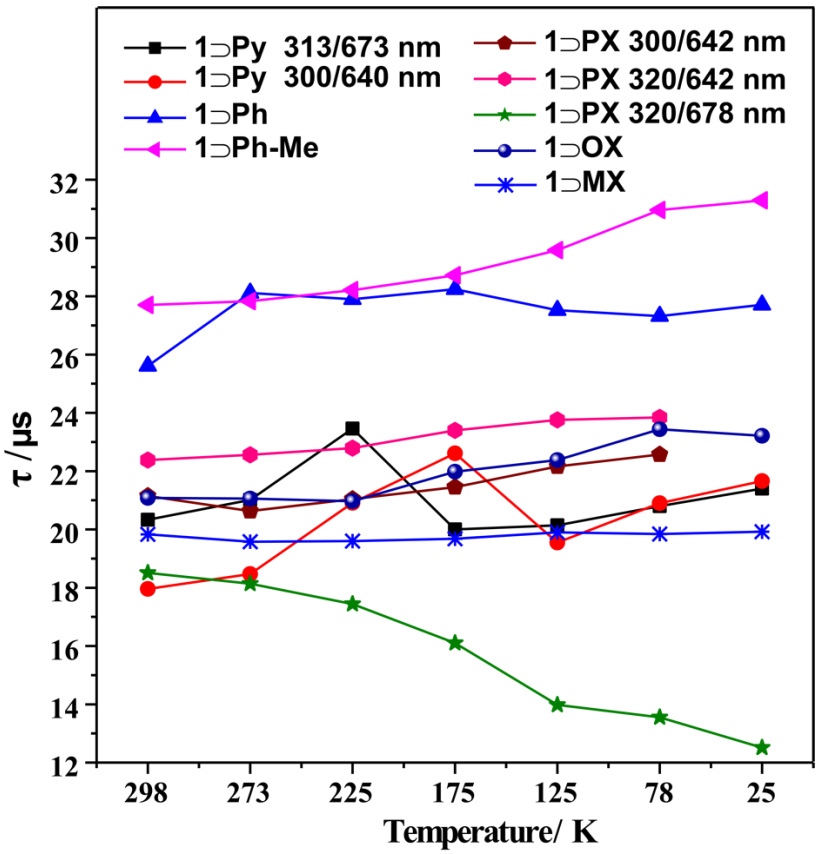

Figure S26. Lifetime data of inclusion complexes at different temperatures. τ is the average lifetime

Computational details

All calculations were performed with Gaussian 09 suit of program[2] employing density functional theory (DFT). The hybrid functional PBE0[3] and double zeta basis set (LanL2DZ[4] for Cu atom and 6-31G(d)[5] for other atoms) was applied here. The geometry of cage host 1 was fully optimized in DCM with PCM solvent model and the crystal structures of inclusion complexes were utilized here. The singlet point energy calculations were done to obtain the electrostatic potential. The maps of electrostatic potential (ESP) surface were obtained from the NBO charge with the isovalue of 0.01 a.u.

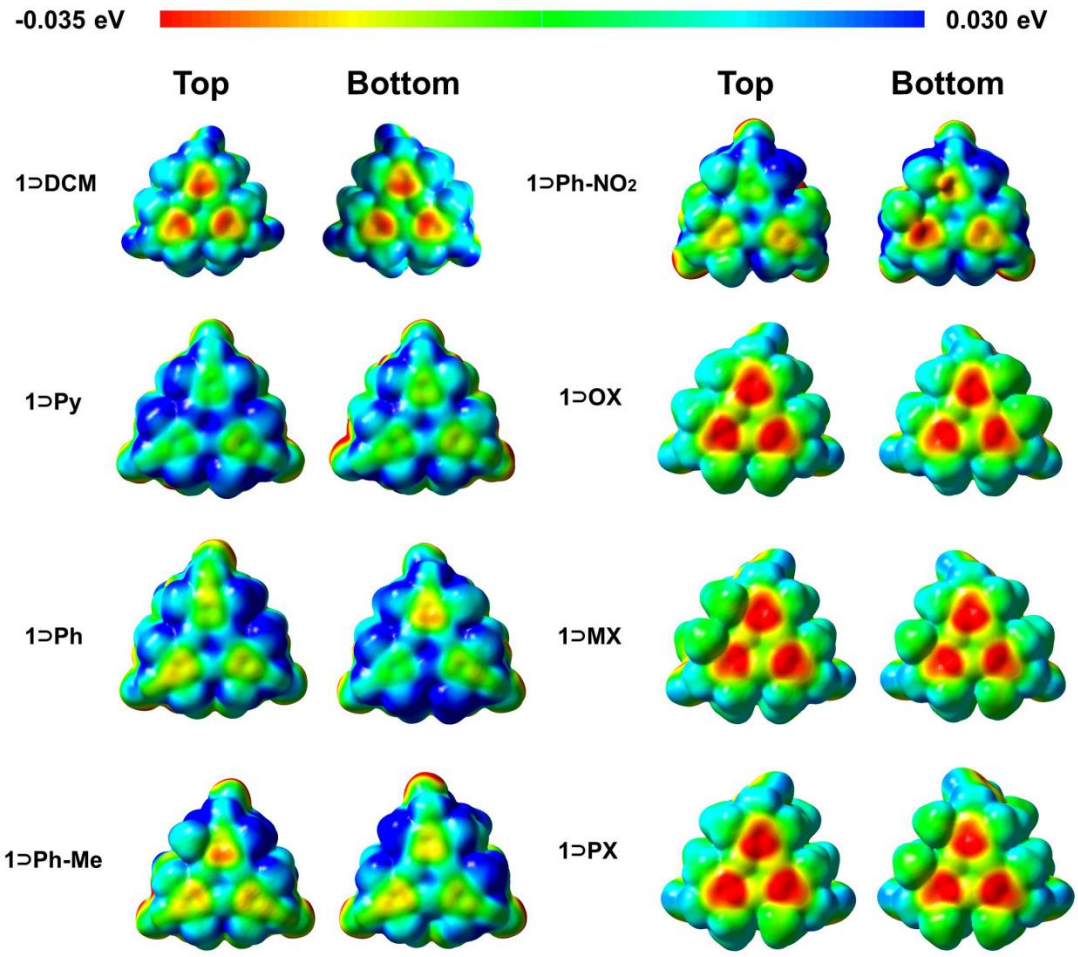

Figure S27. Mapped electrostatic potentials (ESP) of inclusion complexes on the surface with the isovalue of 0.01 a.u.

Table S6. Summary of photophysical parameters for cages in the solid state at 298 and 77 K.

		Ph	Ph-Me	OX	MX
298 K	λ_{ex} (nm)	314	310	305	313
	λ_{em} (nm)	693	681	654	668
	τ (μs)	25.61	1.32 ± 0.19 (0.40 %) 27.81 ± 0.09 (99.60 %)	5.35 ± 0.08 (3.79 %) 21.70 ± 0.13 (96.21 %)	4.06 ± 0.26 (3.05 %) 20.33 ± 0.17 (96.95 %)
	χ^2	1.953	1.572	1.118	0.598
77 K	τ (μs)	6.69 ± 0.75 (2.34 %) 27.80 ± 0.14 (97.66 %)	0.17 ± 0.13 (0.32 %) 31.06 ± 0.02 (99.68 %)	3.06 ± 0.16 (2.80 %) 24.03 ± 0.10 (97.20 %)	3.02 ± 0.11 (3.01 %) 20.36 ± 0.10 (96.99 %)
	χ^2	1.399	1.753	1.265	1.056

Table S7. Selected photophysical parameters for **Py** and **PX** in the solid state at 298 and 77 K.

		Py		PX		
298 K	λ_{ex} (nm)	313	300	300	320	320
	λ_{em} (nm)	673	640	642	642	678
	τ (μs)	3.59 ± 0.17 (2.87 %) 20.68 ± 0.11 (97.13 %)	5.55 ± 0.15 (8.97 %) 19.18 ± 0.23 (91.03%)	4.94 ± 0.19 (5.42 %) 22.08 ± 0.13 (94.58 %)	22.56	2.55 ± 0.14 (5.43 %) 19.43 ± 0.10 (94.57 %)
	χ^2	1.218	1.277	1.396	1.868	1.169
77 K	τ (μs)	5.15 ± 0.12 (4.66 %) 21.56 ± 0.10 (95.34 %)	8.46 ± 0.24 (11.90 %) 22.58 ± 0.32 (88.10 %)	4.54 ± 0.37 (6.94 %) 23.91 ± 0.13 (93.06 %)	1.98 ± 0.27 (2.52 %) 24.40 ± 0.11 (97.48 %)	0.94 ± 0.03 (21.80 %) 17.07 ± 0.16 (78.20 %)
	χ^2	1.474	1.466	1.689	1.902	0.953

7. References

S1. J. A. Aguilar, P. Díaz, A. Doménech, E. García-España, J. M. Llinares, S. V. Luis, J. A. Ramírez, C. Soriano. Synthesis, protonation and Cu^{2+} co-ordination studies on a new family of thiophenophane receptors. *J. Chem. Soc. Perkin Trans.* **1999**, *2*, 1159–1168.

S2. M. J. Frisch, G. W. T., H. B. Schlegel, G. E. Scuseria, M. A. Robb, J. R. Cheeseman, G. Scalmani, V. Barone, B. Mennucci, G. A. Petersson, H. Nakatsuji, M. Caricato, X. Li, H. P. Hratchian, A. F. Izmaylov, J. Bloino, G. Zheng, J. L. Sonnenberg, M. Hada, M. Ehara, K. Toyota, R. Fukuda, J. Hasegawa, M. Ishida, T. Nakajima, Y. Honda, O. Kitao, H. Nakai, T. Vreven, J. A. Montgomery, Jr., J. E. Peralta, F. Ogliaro, M. Bearpark, J. J. Heyd, E. Brothers, K. N. Kudin, V. N. Staroverov, R. Kobayashi, J. Normand, K. Raghavachari, A. Rendell, J. C. Burant, S. S. Iyengar, J. Tomasi, M. Cossi, N. Rega, J. M. Millam, M. Klene, J. E. Knox, J. B. Cross, V. Bakken, C. Adamo, J. Jaramillo, R. Gomperts, R. E. Stratmann, O. Yazyev, A. J. Austin, R. Cammi, C. Pomelli, J. W. Ochterski, R. L. Martin, K. Morokuma, V. G. Zakrzewski, G. A. Voth, P. Salvador, J. J. Dannenberg, S. Dapprich, A. D. Daniels, Ö. Farkas, J. B. Foresman, J. V. Ortiz, J. Cioslowski, and D. J. Fox, Gaussian, Inc., Wallingford CT, Gaussian, Inc.Wallingford CT, 2009.

S3. C. Adamo, V. Barone, Toward reliable density functional methods without adjustable parameters: The PBE0 model. *J. Chem. Phy.* **1999**, *110*, 6158.

S4. C. E. Check, T. O. Faust, J. M. Bailey, B. J. Wright, T. M. Gilbert, L. S. Sunderlin, Addition of polarization and diffuse functions to the LANL2DZ basis set for P-Block elements. *J. Phys. Chem. A* **2001**, *105*, 8111.

S5. P. C Hariharan, J. A. Pople, The influence of polarization functions on molecular orbital hydrogenation energies. *Theor. Chim. Acta* **1973**, *28*, 213.